

Charge-changing processes in small-impact-parameter collisions between O^{+q} and rare gases*

B. Rosner[†] and D. Gur[‡]

Department of Physics, Technion, Haifa, Israel
and Department of Physics, University of Pittsburgh, Pittsburgh, Pennsylvania 15260

(Received 4 August 1976)

We have studied the charge distributions of oxygen ions after small-impact-parameter collisions with Ne, Ar, Kr, and Xe gases. Bombarding energies in the 10–30-MeV range and incoming charge states between 4^+ and 7^+ were scattered to angles between 5° and 8° in a single collision process. The measurements indicate that for the heavier gases an equilibrium charge distribution is obtained after a single collision. Interpretation of the experimental results on the basis of a statistical “compound-atom” model is suggested.

INTRODUCTION

In the collision process between fast-moving heavy ions, part of the kinetic energy is usually transferred to their electrons, causing excitation, ionization, and transfer of electrons between the projectile and target atoms. Two major mechanisms govern these charge-changing processes: the direct Coulomb interaction¹ and the Pauli interaction.² The relative importance of the two mechanisms can be described using the following parameters: v_i —the relative velocity between the colliding atoms, and d —the distance of closest approach in the collision.

The first mechanism, namely the direct Coulomb interaction, operates between the respective electron clouds as well as between the nuclear charge and the electrons. It may be considered a binary interaction and becomes the dominant process when

$$v_i > v_e, \quad (1)$$

$$d \approx R_e, \quad (2)$$

where v_e is the orbital velocity of the interacting bound electrons and R_e the radius of their orbitals.

The Pauli interaction is due to the fact that the collision occurs between two systems of fermions, which results in some overlap between them; thus some rearrangement of the energy levels of both systems is needed. During the rearrangement time the energy transferred to the electronic orbitals may sometimes be quite large, and as the colliding ions fly apart, electrons can easily be left in excited states, ejected, or transferred between the colliding partners. Such interactions are described very well by the molecular orbitals model,³ and it is the dominant process when

$$v_i < v_e, \quad (3)$$

$$R_2 < d < R_1, \quad (4)$$

where R_1 and R_2 are the radii of two electronic orbitals.

The situation in the present experiment differs from the above-mentioned cases. Owing to the high bombarding energy of the projectile and the large scattering angles, we have a case in which the distance of closest approach is much smaller than both K -shell radii of the projectile and target atoms. On the other hand, v_i is greater than the velocities of all orbital electrons of the projectile and of most of those belonging to the target. We may therefore expect some new phenomena⁴ due to the fast and almost complete overlap of the two colliding electronic clouds.

EXPERIMENTAL

Oxygen beams in the 10–30-MeV energy range with initial charges 4^+ , 5^+ , 6^+ , and 7^+ were obtained from the three-stage tandem accelerator of the University of Pittsburgh and scattered to angles between 5° and 8° by single collisions with Ne, Ar, Kr, and Xe gases contained in a windowless gas target. The target was in the form of a hollow cylinder 25 mm in diameter. It had a 3-mm circular hole for the beam to enter and a 3 by 5 mm slot for the scattered beam to emerge. The cylinder was mounted in the center of the scattering chamber of the split-pole magnetic spectrograph. Gas was continuously leaked into the cell to maintain a typical thickness of about 10^{13} atoms/cm³ ($P = 4 \times 10^{-4}$ Torr). The high-speed vacuum pumps were able to maintain the vacuum throughout the system to pressures below 4×10^{-6} Torr while the pressure in the scattering chamber was usually at 5.10^{-5} Torr.

Five outgoing charges, $4^+ - 8^+$, were detected simultaneously by five position-sensitive detectors mounted on the focal plane of the spectrograph. By doubling the magnetic field of the spectrograph, the $2^+ - 4^+$ outgoing charges were detected without any need for changes in the geometry of the setup. The choice of position-sensitive detectors rather than ordinary solid-state detectors was made to ensure that the outgoing charges hit their center

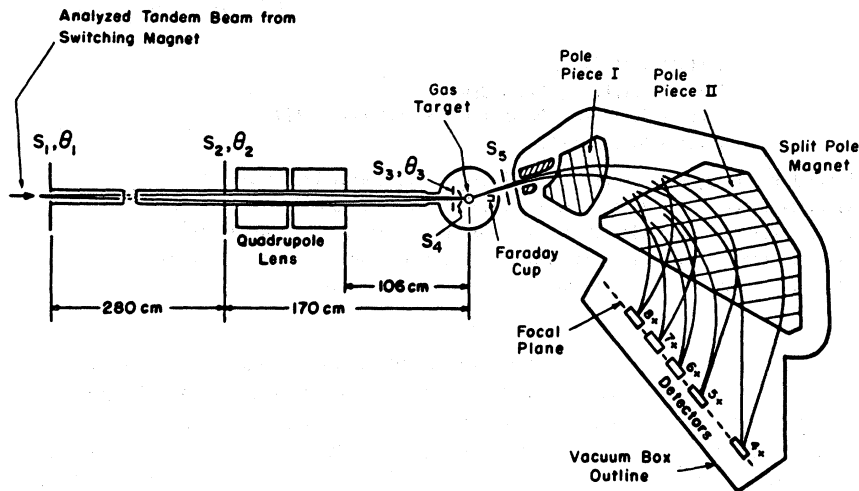


FIG. 1. Schematic layout of the experimental setup.

position with no losses. The single narrow peak observed in the position spectrum verified the purity of the target gas. Owing to the rather low cross section expected for scattering to large angles in a single collision, thin solid targets were used to find the exact locations in which the detectors were to be mounted. A general view of the experimental setup is given in Fig. 1. The beam enters from the left after charge analysis by a switching magnet. Additional analysis is made by the set of quadrupole lens before hitting the target.

The position signals from the five detectors were analyzed and stored, using a PDP-15 computer to obtain the relative intensities of the various outgoing charge states. No attempt to obtain absolute cross sections was made in the experiment.

The single collision nature of the experiment was tested by the following three tests: (1) The purity of the incoming charge state was determined as a function of the gas pressure with the spectrograph set at 0° . Gas was leaked directly into scattering chamber with no target in position and the distribution of the incoming charges was measured by the position-sensitive detectors in the spectrograph. Figure 2 presents the results obtained for a 6^+ incoming charge at 30 MeV. At the working pressure, namely 5×10^{-5} Torr in the scattering chamber, only about 0.2% of charges 5^+ and 7^+ occurred in the beam. The intensity of these impurities increase as a function of the pressure but remain below 1% even for pressures four times higher. Extrapolation to zero pressure gives an indication of the small contribution of the slit scattering. Similar tests were made for other incoming charges and other bombarding energies. But even for extreme cases such as

charge 4^+ at 30 MeV for example, the impurities of charges 5^+ and 6^+ were found to be less than 5%.

(2) To ascertain the single collision in the gas target, the outgoing charges scattered to $\theta = 5^\circ$ were measured as a function of the pressure up to twice the working pressure. It was found that the total yield increased linearly with the pressure while no significant changes could be observed in the relative intensities of the outgoing charges.

(3) The possibility of additional charge exchanges on the flight path between the target and the detector due to the residual pressure in the magnetic spectrograph was checked as follows: The outgoing charge states distribution for the oxygen ions after traversing through a thin solid target was determined with the best vacuum conditions. Later, gas was leaked into the scattering chamber and the outgoing charge distribution was again measured as a function of the pressure. No noticeable changes either in the sum of all the charge states

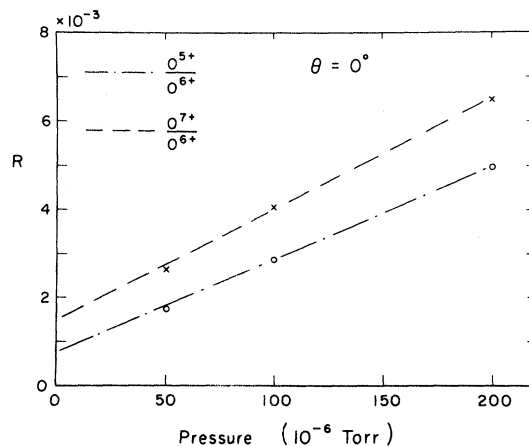


FIG. 2. Impurity of incoming charge states as a function of pressure for 30-MeV 6^+ oxygen projectiles.

as detected by the five detectors or in their relative intensities was found, up to twice the working pressure, within a statistical accuracy of 0.5%. As the equilibrium charge-state distribution in solid is higher compared to gas, these results prove that no additional charge exchange occurred either in the field-free region between the target and the detectors or in the flight path through the magnetic field of the spectrograph.

RESULTS

The angular distribution of four outgoing charges, namely $5^+ - 8^+$, taken in the angular range of $5^\circ - 8^\circ$ at a bombarding energy of 24 MeV on Kr target is shown in Fig. 3. The similarity of the shapes of these distributions is very clear. This insensitivity of the charge-state distribution to the scattering angle is quite contradictory to the results obtained in similar experiments done at lower bombarding energies with many different projectile-target combinations.⁵ In those experiments which were done by the Everhart group,⁶ the Afrosimov group,⁷ and others,⁸ it was usually found that for larger scattering angles which correspond to deeper penetration into the atomic shells, the average charge increases sometimes monotonically or in steps, as more electronic orbitals are crossed. In fact, the unexpected results in the present experiment, which is a typical result for an "equilibrium charge distribution," stressed the need to ensure that we have really a single-collision experiment. At this stage the three tests mentioned

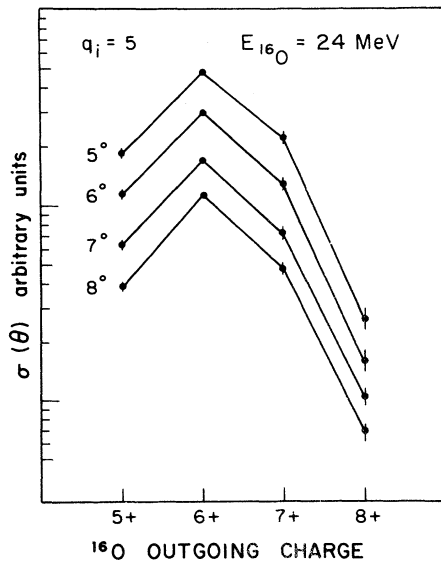


FIG. 3. Charge distribution of the oxygen projectile after scattering by a single collision by Kr at the bombarding energy of 24 MeV.

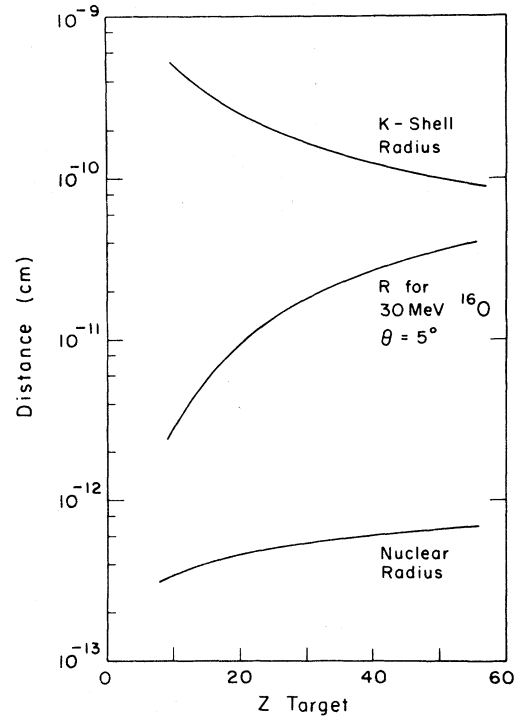


FIG. 4. Radius of K -shell electrons, nuclear radius, and distance of closest approach for 30-MeV oxygen ions to different atoms.

in the previous section were devised and very carefully performed.

However, this insensitivity shown in Fig. 3 can be readily explained by simple considerations based on the geometry of the collision. In Fig. 4 we have plotted the radius of the K -shell, the nuclear radius and the distance of closest approach calculated for 30-MeV oxygen ions scattered to 5° by different elements. It is clear that even for the Xe target ($Z = 54$), a 30-MeV oxygen projectile scattered to $\theta = 5^\circ$ penetrates twice as deeply as the K -shell radius of the target, and much more so for Kr, Ar, and Ne targets. Thus an increase of the scattering angle beyond 5° does not correspond to penetration of any new shells, and as a matter of fact does not change very much the overlap of the two electronic clouds. On the other hand the distance between the atomic nuclei is still far beyond the range of nuclear forces.

The most interesting and unexpected results of this study were the insensitivities of the outgoing charge-state distribution on the value of the incoming charge, especially in high- Z targets. This is shown in Fig. 5. The figure presents the outgoing charge distribution of 30-MeV oxygen ions after a single collision with four different gas targets. The initial charge states of the projectile ranges between $q_i = 4^+, 5^+, 6^+,$ and 7^+ . In Table I

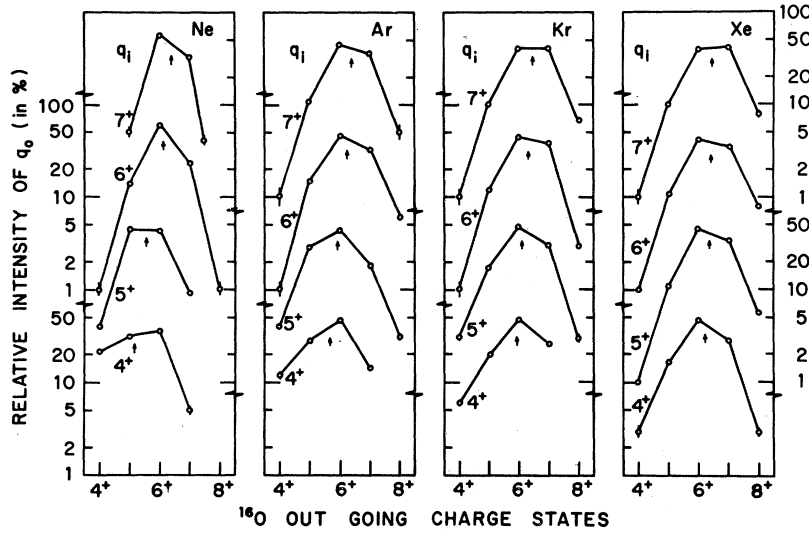


FIG. 5. Charge-state distributions of outgoing 30-MeV oxygen ions as a function of their initial charge q_i , after scattering at $\theta = 5^\circ$ by Ne, Ar, Kr, and Xe atoms.

we give the average values of the charge distribution for all bombarding energies and targets used in the present experiment. The results given in this table show increasing independence of the average outgoing charge $\langle q_0 \rangle$ on the initial charge q_i as the atomic number of the target gas increases. This was found to be true for all the bombarding energies. For the lighter targets, neon for example, a change of 3 units in q_i at 30-MeV bombarding energy results in a change of 1.2 units in $\langle q_0 \rangle$. The same change in q_i results in a change of

only 0.27 units in $\langle q_0 \rangle$ when the target gas is xenon. A graphical presentation of these results is displayed in Fig. 6 for the 30-MeV bombarding-energy case. A somewhat more illustrative picture proving the above-mentioned conclusion can be obtained when the same data are plotted for a given center-of-mass energy. This is shown in Fig. 7 for $E = 15$ MeV. None of the experiments was done exactly at this center-of-mass energy, but the interpolations needed to construct it from the data did not exceed a few MeV. The physical reasons to justify a center-of-mass presentation are not clear, however Fig. 7 shows clearly that for lighter targets the outgoing oxygen projectile still "remembers" its original initial charge, but

TABLE I. Summary of values of average outgoing charge states $\langle q_0 \rangle$ obtained in the present experiment.

q_i	Ne	Ar	Kr	Xe
$E = 30$ MeV				
4^+	5.15	5.67	5.91	6.21
5^+	5.55	5.90	6.13	6.39
6^+	6.09	6.28	6.31	6.41
7^+	6.35	6.35	6.45	6.48
$E = 25$ MeV				
4^+	5.09	5.48	5.90	6.09
5^+	5.59	5.71	6.08	6.19
6^+			6.23	6.29
$E = 20$ MeV				
4^+	5.09		5.77	6.04
5^+	5.46		5.88	6.13
$E = 15$ MeV				
4^+			5.50	5.78
5^+			5.56	5.87
6^+			5.63	5.97
$E = 10$ MeV				
3^+	4.61	4.94		5.54
4^+	5.02	5.15		5.60

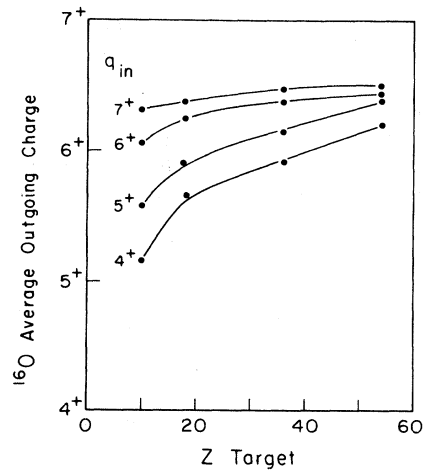


FIG. 6. Average outgoing charge of the 30-MeV oxygen projectiles after scattering by a single collision by Ne, Ar, Kr, and Xe atoms.

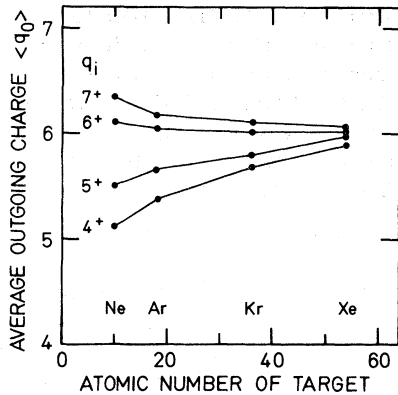


FIG. 7. Similar to Fig. 6. Plotted for oxygen projectiles with $E_{cm} = 15$ MeV.

for very heavy targets this memory will be completely lost.

DISCUSSION

Both above-mentioned experimental results, namely the similarity of the outgoing charge distribution at all measured scattering angles and especially the systematic trend towards the independence of those distributions on the incoming charge of the oxygen projectile as the target atoms get heavier, indicate that the charge-changing processes which are dominant for collisions with large impact parameters (0° scattering) do not play an important role in the present study. In the latter case which is governed by the Coulomb interactions, the target cross sections are usually those describing the stripping and pickup of a single electron. They become quite small for multiple-electron transfers. In addition these cross sections are very strongly angle dependent. Both of those predictions are certainly in a very bad agreement with the observations in the present study.

The use of the Pauli interaction which is equivalent to the removal of electrons by the promotion process³ is inadequate in the analysis of the present experiment because the velocity of the projectile is larger than the orbital velocities of most of the bound electrons in the colliding system. This can be readily seen from the level diagrams given in Fig. 8. Here we display the binding energies of the electrons of the projectile and the four target atoms. Roughly speaking, electrons which are bound by less than 750 eV have orbital velocities smaller than the velocity of the 30-MeV oxygen ion. These are all the electrons of the projectile and of the neon target, and most of the electrons of the heavier target atoms. Thus the diabatic collision model is inadequate in the present case.

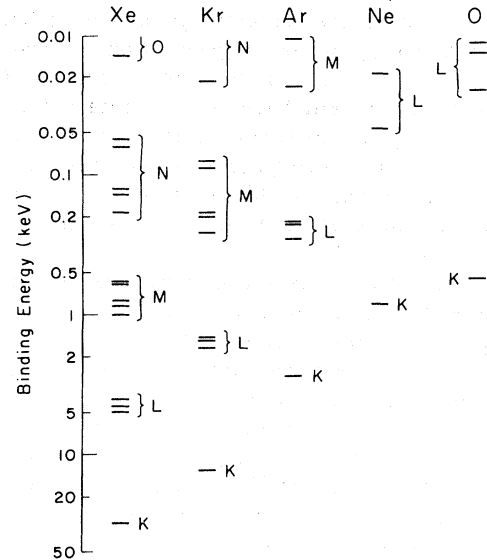


FIG. 8. Binding energies of the electrons of O, Ne, Ar, Kr, and Xe atoms.

Furthermore it is not plausible that the molecular-orbital model,⁹ which takes into account the microscopic structure of the target, will be able to describe the experimental results because the microscopic details of the four systems such as number of electrons, binding energies, radii of orbitals are very different whereas the experimental results are quite similar in all cases.

An alternative approach to the interpretation of the experimental results may be based on a statistical model.¹⁰ As the swift projectile penetrates deeply through the electronic orbitals of the target atom all energy levels interact and for a short period all electrons and excitation energies are shared by the two colliding partners. This may resemble the formation of a compound nucleus,¹¹ which is the most probable result of a nuclear interaction for collisions with impact parameter smaller than the nuclear radius. In this sense the outgoing channels are decoupled from the incoming one. As most of the electrons in the system belong to the target atom, the charge brought in by the projectile does not appreciably affect the statistical equilibrium which finally determines the charge distribution of the outgoing ions. Thus for atomic collisions with small impact parameter an equilibrium charge distribution may be reached right after a single collision.

The analogy with the compound-nucleus picture should be taken with caution. The nuclear forces and the electromagnetic forces have very little in common. The first one is short range and very strong, whereas the second is a long-range force and much weaker. In the nuclear case most of the

kinetic energy of the projectile is converted into excitation energy of the compound system, whereas only a small part of it is inelastically scattered in the atomic case. Furthermore, the interaction times involved are also very different in both cases. We have therefore two quite different physical mechanisms which, due to the statistical approach needed in their evaluation, happen to yield somewhat similar results.

The final-charge-state distribution as measured by the detectors is affected by additional loss of electrons: the Auger effect. The projectile, and to some extent the target atom too, may lose a considerable number of electrons after separation. Many electrons may be left at higher excitations, and when they decay to their ground states, Auger electrons may be emitted especially in light elements. This effect will increase the average value of the outgoing charge distribution and will have to be taken into consideration when quantitative calculation will be underway.

The insensitivity of the outgoing to the incoming charge state can be envisaged in a somewhat more quantitative way based on Bohr theory.¹² Equilibrium-like conditions in a single collision can be realized if the probabilities of loss P_l and capture P_c for most of the electrons in the colliding system

are near unity. For 30-MeV O-Kr for example and scattering angle of 5° we have a distance of closest approach nearly 0.003 a.u. compared to the K -shell radius of Kr (0.03 a.u.) and of O (0.12 a.u.). The cross section for loss and capture of electrons for such deep penetration between heavy ions is given by the symmetric expression

$$\sigma_l \sim \sigma_c \sim \pi a_0^2 (Z^{1/3} + Z_T^{1/3}) (v_0/v)^2,$$

where v is the c.m. projectile velocity and v_0 the electrons' orbital velocity. For most of the electrons, namely the M - and N -shell electrons of the target and all electrons of the projectile, $v > v_0$. Thus we are at the maximum of the ionization, and the probability of ionizing the electrons in our small-impact-parameter collision is practically unity.

ACKNOWLEDGMENTS

The authors are grateful to Professor J. X. Saladin for his constant interest in this study, to Professor Q. C. Kessel, Professor A. Weidenmüller, and Professor H. D. Betz for most helpful discussions and to J. Alessi, K. C. Chan, and L. Shabason for their help in performing the experiment.

*Supported by the National Science Foundation.

†Partly supported by G. S. I. Darmstadt Foundation.

‡Present address: Radiation Center, Presby. Hospital, Pittsburgh, Pa. 15261.

¹Hans-Dieter Betz, *Rev. Mod. Phys.* **44**, 465 (1972).

²J. D. Garcia, R. J. Fortner, and T. M. Kavanagh, *Rev. Mod. Phys.* **45**, 111 (1973).

³U. Fano and W. Lichten, *Phys. Rev. Lett.* **14**, 627 (1965); W. Lichten, *Phys. Rev.* **164**, 131 (1967).

⁴B. Rosner, D. Gur, J. Alessi, K. C. Chan, and L. Shabason, *Phys. Lett.* **57A**, 320 (1976).

⁵Q. C. Kessel and B. Fastrup, *Case Stud. At. Phys.* **3**, 207 (1972).

⁶E. Everhart and Q. C. Kessel, *Phys. Rev.* **146**, 16 (1966).

⁷V. V. Afrosimov, Yu. S. Gordeev, M. N. Panov and N. V. Fedorenko, *Zh. Eksp. Teor. Fiz. Pis'ma Red.* **2**, 291 (1965) [*JETP Lett.* **2**, 185 (1965)].

⁸B. Rosner, D. Gur, and Y. Dar, *Bull. Israeli Phys. Soc.* **20**, 27 (1974).

⁹M. Barat and W. Lichten, *Phys. Rev. A* **6**, 211 (1972).

¹⁰E. Everhart and Q. C. Kessel, *Phys. Rev.* **146**, 27 (1966); M. H. Mittleman and L. Wilets, *Phys. Rev.* **154**, 12 (1967); A. Russek and J. Meli, *Phys. (Utr.)* **46**, 222 (1970).

¹¹V. F. Weisskopf and D. H. Ewing, *Phys. Rev.* **57**, 472 (1940).

¹²N. Bohr, *K. Dan. Vidensk. Selsk. Mat.-Fys. Medd.* **18**, No. 8 (1948).